Compact massive MIMO antenna array for small 5G base stations

Muhammad Ali

School of Electrical Engineering

Thesis submitted for examination for the degree of Master of Science in Technology.

Espoo 31.3.2016

Thesis supervisors:

Prof. Katsuyuki Haneda

Thesis advisor:

D.Sc. (Tech.) Linsheng Li

Aalto University
School of Electrical
Engineering

AALTO UNIVERSITY
SCHOOL OF ELECTRICAL ENGINEERING

ABSTRACT OF THE
MASTER'S THESIS

Author: Muhammad Ali

Title: Compact massive MIMO antenna array for small 5G base stations

Date: 31.3.2016 Language: English Number of pages: 6+33

Department of Radio Science and Engineering

Professorship: Antenna Design

Supervisor: Prof. Katsuyuki Haneda

Advisor: D.Sc. (Tech.) Linsheng Li

This master's thesis introduces a massive MIMO antenna array that operates at 5 GHz and 15 GHz. The array has a wideband input matching response and a low coupling level between antennas.

Multiple designs have been introduced to match the design goals. Parametric studies were performed using EM simulation to optimize the design. A prototype of the reference design has been fabricated and measured.

The prototype was measured for input matching level and coupling. Moreover, the radiation patterns were measured in the anechoic chamber. The reference design provided a bandwidth of 230 MHz for - 6 dB response. Mutual coupling between elements was $\leq$ -10 dB according to the design goal. The size of the manufactured prototype fit the design requirement in terms of number of antenna elements in the given dimensions.

Keywords: Antenna array, bandwidth, input matching, massive MIMO, mutual coupling, patch antenna, polarization, radiation pattern

Preface

This master's thesis is based on research work conducted at the Department of Radio Science and Engineering (RAD) at Aalto University, School of Electrical Engineering. Throughout the research progress and thesis writing, many people had important inputs that contributed to accomplish this work.

First, I would like to express my gratitude to my advisor Dr. Linsheng Li, for displaying a high level of academic and professional attitude through his instructions and coaching. His wide knowledge in the research field in both theory and practice, created a very fruitful work experience for me. Secondly, I would like to thank my supervisor Prof. Katsuyuki Haneda for giving me the opportunity to exploit my potential through this thesis topic, and his sharp and constructive feedback throughout the thesis work, and being such good role model for professionalism.

I would like to thank Dr. Jari Holopainen, Dr. Clemens Icheln, Prof. Antti Räisänen, Prof. Ville Viikari, Mr. Mikko Heino and Mr. Gaurav Khairakar for their comments and constructive suggestions regarding the antenna design and simulation. In addition, Mr. Usman Virk for helping me conducting the measurements. I would like also to thank Dr. Kari Stadius from department of Department of Micro- and Nanosciences at Aalto university for supplementing our measurements with the department equipment.

I have special thanks to my teacher Prof. Hany Hammad from my home university, for his great influence through his teachings and materials, that I have kept referring to and studying from through out my master's studies. Most of all his, guidance and coaching that defined and highlighted my whole career path.

I would like to thank my family, especially my mother Dr. Iman Khattab for believing in me and supporting me without questioning. Also my sisters for their immense emotional support through out my thesis work.

Above all, I would like to thank God almighty, for his blessings and support, through awarding me this opportunity in such a great institution and for providing me with the strength to proceed forward and a positive experience.

Otaniemi, 31.3.2016

Muhammad Ali

Contents

Symbols and abbreviations

Symbols

ϵ_r	Relative permittivity
λ_0	Guided wavelength$[m]$
h/λ_0	Normalized substrate thickness
θ	elevation angle [°]
φ	azimuthal angle [°]

Abbreviations

%BW	Relative bandwidth
CST	Computer simulation technology, an electromagnetic simulated software
CP	Circular polarization
EM	Electromagnetic
IF	Intermediate frequency
MC	Mutual coupling
MEA	Multiple antenna elements
MIMO	Multiple-input-multiple-output
MISO	Multiple-input-single-output
MWS	Microwave Studio, an electromagnetic simulation software by CST
S-parameters	Scattering parameters
SIMO	Single-input-multiple-output
SNR	Signal to noise ratio
TM	Transverse magnetic
VSWR	Voltage standing wave ratio
WLAN	Wireless local area network

1 Introduction

1.1 Motivation for massive MIMO antenna array

As 5G technology is looking forward for a more advanced communication, this creates a huge shift in the required data rates for future transmission. The main challenge that bottleneck the shifts to higher data rates is the physical resources described as radio spectrum which usually strictly regulated.

In order overcome such a bottleneck new approaches have been developed to deliver more degree of freedom in the allocated spectrum bandwidth. One of the main approaches is to utilize the wave propagation properties such as multipath. Multipath can be exploited through multiple-input and multiple-output (MIMO) antenna system. The main advantage of MIMO is that the channel capacity scales with the number of antenna elements linearly. Fig. 1 (M: number of antennas, H: channel matrix) displays the difference in the theoretical scaling trend between traditional SIMO/MISO systems versus MIMO. Fig. 1 shows how a higher channel capacity can be achieved through MIMO for the same number of SIMO/MISO antenna elements.

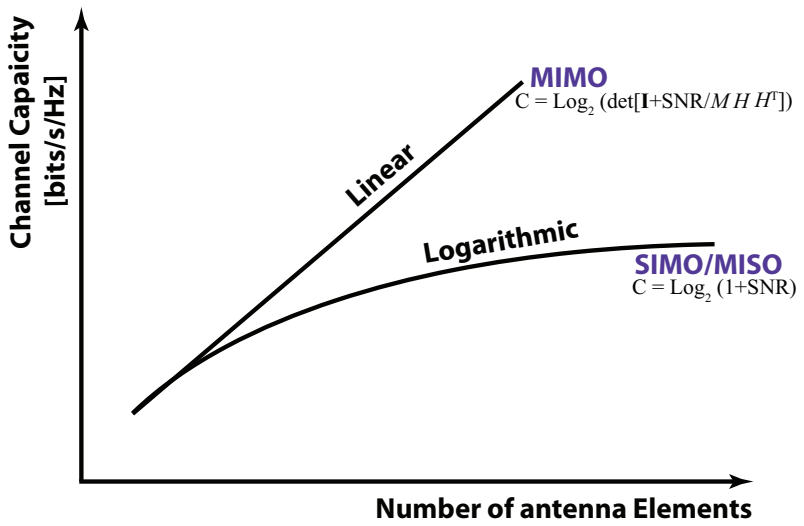

Figure 1: Channel capacity vs. Number of antenna elements [1].

Different architectures have been developed for MIMO technology which utilize multipath propagation with certain hardware constraints [2], they can be summarized as follow:

1.1.1 Point to point MIMO

Point to point MIMO architecture is implemented by equipping the base station with an antenna array (M antenna elements) that supports an end user with an antenna array (k antenna elements)as shown in Fig.2 . The main challenge for this architecture is the scalability, according to the current wireless standards, for

8021.11c it cannot support a system that goes beyond 8×8 as the environment may not support eight data streams as well as the line of sight requirements. This particular design requires high digital processing at both ends of communication.

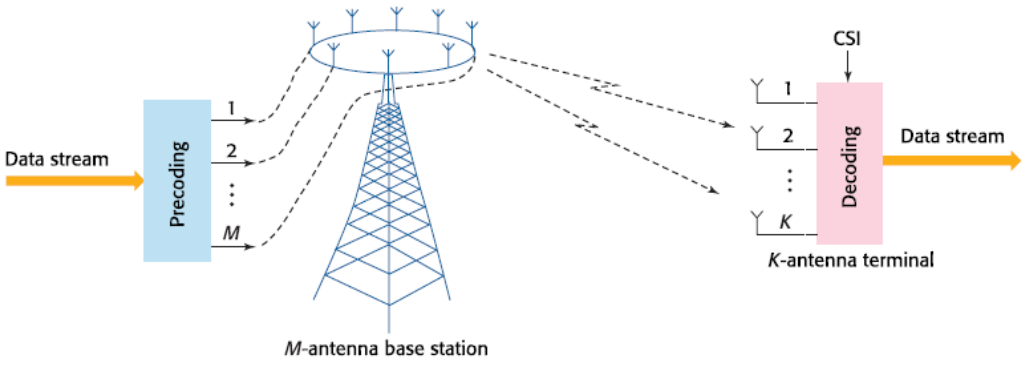

Figure 2: Point to Point MIMO [2]

1.1.2 Multi user MIMO

Multi user MIMO modify the idea of point to point by replacing the single terminal user of k elements array into k users with a single antenna each. This design is better than the single point in terms of providing sufficient number of parallel data streams over the propagation channel due to wider distribution of multiple antennas over space. The main problem of multi user MIMO is that it needs to use a dirty paper coding/decoding, which complexity grows exponentially [2] and in returns limits the overall performance to reach the theoretical shannon limit. Fig.3 displays the Multi user MIMO system.

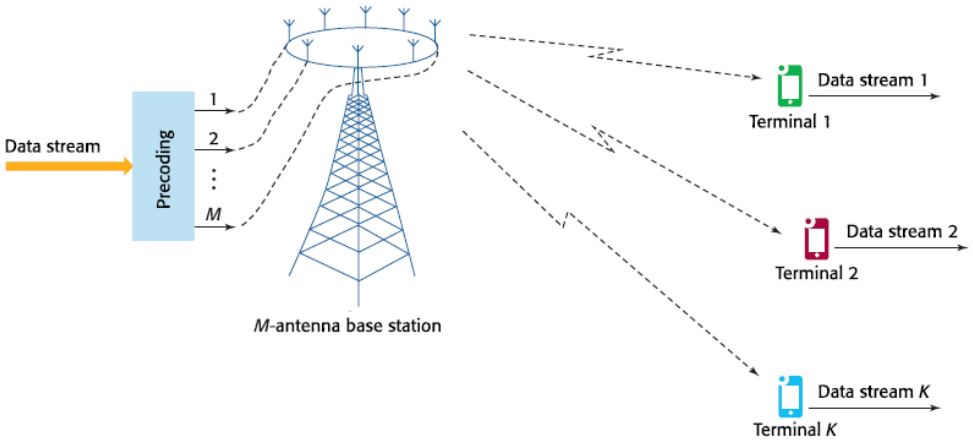

Figure 3: Multi user MIMO [2]

1.1.3 Massive MIMO

The massive MIMO architecture is based on Multi user MIMO in terms providing parallel data stream, in the case of massive MIMO the number of antenna array elements is maximized with a simpler precoding multiplexing. Theoretically as the number of base station antennas increase this precoding algorithm can reach Shannon limit [2]. Fig. 4 shows the downlink of massive MIMO; the signal is precoded and transmitted through a massive antenna array on the base station as on the terminal side there are single k number of users with a single antenna each.

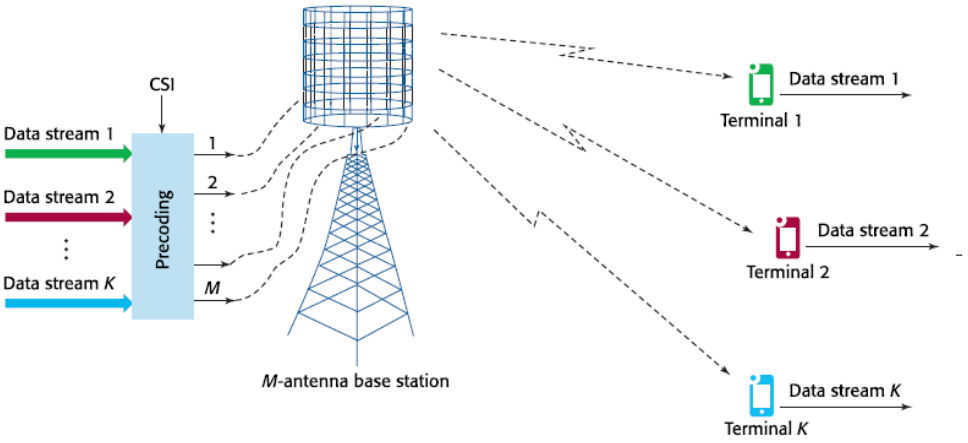

Figure 4: Massive MIMO downlink [2]

1.2 Technical challenges

Scaling massive MIMO system is based on packing the highest number of antenna elements on the desired space, trying to reach Shannon limit. However, the main challenge of packing a high number of antenna elements is to keep the mutual coupling (MC) level practical in reference to the required application of the antenna array. The coupling level and the target design space decides the distance between antenna elements and hence; it decides the maximum number of antenna elements in the array.

In general, for MIMO systems the mutual coupling effect on the capacity is controversial as shown in [3] for using multiple element antennas (MEA) as in MIMO, the mutual coupling have a positive effect on the capacity as it produce a decorrelating effect on the channel coefficients and hence enhance the channel capacity. This happen through pattern diversity as a result of distortion of radiation patterns due to mutual coupling, this claim is also supported by [4]. However, in [5] the results shows that MC will increase the correlation of the elements which lead to reduced capacity for MIMO channel. The conclusion can be drawn from [6] as it states that the MC effect on channel capacity for MIMO is related to the propagation environment, as MC has a positive effect on channel capacity in case of highly correlated environment

and reduce the channel capacity in case of low correlated propagation environment. Moreover, an insight of MEA design for MIMO in reference to channel capacity is presented in [7].

The second main technical challenge is in terms of fabrication; as the in simulation the feeding port are placed as close as possible to guarantee more antenna elements number, or in other case to have dual polarization states, it is challenging after fabrication to feed such ports because the commercial connectors are standardized in terms of size and in some cases the sizes are impractical to be placed next to each other.

To have a dual band antenna element/unit with a high frequency ratio (frequency ratio = f_{high}/f_{low}) ≥ 3 for microstip patch antennas is challenging in terms of optimizing substrate height to achieve the targeted bandwidth for both bands and to guarantee a radiating element at the higher frequency (f_{high}).

1.3 Goal of the thesis

The main goal of the thesis to develop a compact dual band, dual polarized patch antenna array. A size limit of 150 mm $\times$ 180 mm as to function in small base stations and also to resemble the common WLAN (wireless local network) access points size.

The antenna element/unit should operate at two frequency bands; 5.4 GHz and 15 GHz. The 5.4 GHz is chosen to cover the 5 GHz WLAN applications. Both bands should have an input matching of ≤ -6 dB over a bandwidth of 320 MHz. The coupling level between any two antenna elements should be ≤ -10 dB at the bands of interest (input matching bands).

Furthermore, the design should be dual polarized; it can be excited in two different polarization sates. Either the same element/unit itself is dual polarized or the array elements have different polarization scheme.

The designed antenna array should have at least 32 elements/units allocated in the predefined space (150 mm $\times$ 180 mm) and should acquire the desired coupling level (≤ -10 dB).

To conclude, the design goals for the thesis can be summarized as follow:

1. The antenna array should operate at 5.4 GHz and 15 GHz.
2. The input matching should be ≤ -6 dB over a bandwidth of ≥ 320 MHz.
3. The coupling level between any two elements should be ≤ -10 dB.
4. The array should accommodate ≥ 32 elements in a spacing of 150 mm $\times$ 180 mm.

1.4 Overview of the thesis

Chapter 2 of the thesis provides a background on patch antenna including theory of operation, limitations and design diversity.

Chapter 3 displays the design of antenna array. It starts with describing the methodology of simulation and coordination system. The chapter provides a reference design and an improved design which fulfill the design goals.

Chapter 4 illustrates the measurements results of the fabricated reference design. S-parameter results and radiation patterns are presented.

Thesis outcomes are reported and concluded and the also future work related for further improvements is summarized.

2 Background

Patch antenna is adopted in this design due to its low profile which is necessary for a compact design. Section 2.1 will give a brief introduction the basic theory of patch antennas, limitation and diversity. Section 2.2 will present paper survey conducted to demonstrate the recent massive MIMO patch antenna arrays.

2.1 Patch antennas

The concept of microstrip radiators was patented in 1955 [8], but the practical development happened in the 1970's as good substrates availability arose [9], which guarantee a low cost, low volume and light weight for the designs. A microstrip antenna in its simplest form is a radiating conductor (copper or gold) on one side of a substrate and a ground plane on the other side. The radiating conductor can be any shape as shown in Fig. 5 but uniform shapes are considered and adopted.

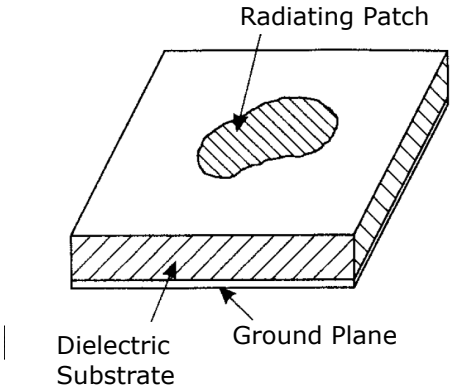

Figure 5: Patch antenna structure [9]

2.1.1 Theory of operation

The patch antenna can be analyzed through two different models [9]. The first model is a radiating microstrip line, Fig. 6 (a) as the radiating element is charged in opposite charge of the ground plane, this induces surface currents at the edges which is responsible for fringing fields as the source of radiation. The second model 6 (b) is the cavity model with TM_{100} mode, the four walls of the cavity are represented as small apertures in this case they are the source of the radiation.

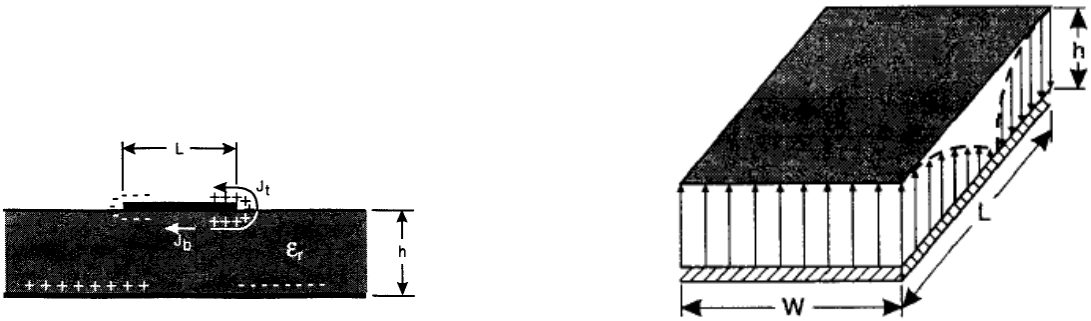

(a) Radiating microstrip line model

(b) Resonating cavity model

Figure 6: Patch antenna analysis models. [9]

2.1.2 Substrate selection

To design a microstrip patch antenna the first criteria is to choose a suitable dielectric substrate. The main two factors that defines the antenna performance are the dielectric constant ϵ_r and the height (thickness) of the substrate h. Although a thicker substrate will provide a better impedance bandwidth response (will be discussed in the upcoming subsection) and a better radiated power. However, it will induced more dielectric losses and surface wave losses. On the same hand, the dielectric constant ϵ_r affects the performance at the same level, whereas a low value of ϵ_r will increase the radiated power, however the size of the antenna increases. As the loss tangent of the substrate increases, the dielectric losses increases and reduces the antenna efficiency [9].

2.1.3 Bandwidth

Although the patch antenna introduce a compact design solution, however it possesses a narrow band input matching response. For simplicity the patch antenna can be modeled as a parallel plate capacitor with capacitance C shown in equation 1, where A is the area of the plate and d is the distance between the plates in meters. The bandwidth can also be expressed as $1/Q$ where Q is the quality factor. The quality factor of the capacitor is shown in equation 2. In conclusion, as the capacitance increase the quality factor decreases and hence the bandwidth increases. So, to have a wider bandwidth a trade off between the dielectric constant and the height of the dielectric should be optimized for the application.

$$C = \epsilon_r \frac{A}{4\pi d} \tag{1}$$

$$Q = \frac{1}{2\pi f C} \tag{2}$$

Bandwidth can have different definitions, one of them is the percentage bandwidth as shown in equation 3, where f_H is the highest band frequency, f_L is the lower band

frequency and f_c is the center frequency. And as shown from the equation the higher frequencies have a wider bandwidth as f_c has bigger values.

$$\%B.W = \frac{f_H - f_L}{f_c} \times 100 \tag{3}$$

Fig. 7 shows the relationship between percentage bandwidth $B.W(\%)$ and frequency for a substrate of $\epsilon_r = 2.33$.

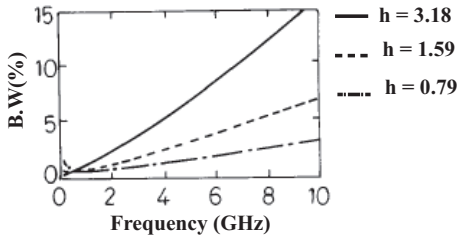

Figure 7: Relative bandwidth versus frequency for $\epsilon_r = 2.33$ with three different substrate heights h (mm) [10].

However, increasing the frequency does not guarantee a functioning antenna as the high frequencies have higher attenuation and hence the thickness of the substrate will attenuate the signal and reduce the efficiency. Fig. 8 shows the efficiency percentage as a function of normalized substrate thickness, which is the ratio between the substrate height h and operating wavelength λ_0 for different dielectric constants ϵ_r. The higher h/λ_0 value the lower the efficiency even if it has a wider impedance matching bandwidth.

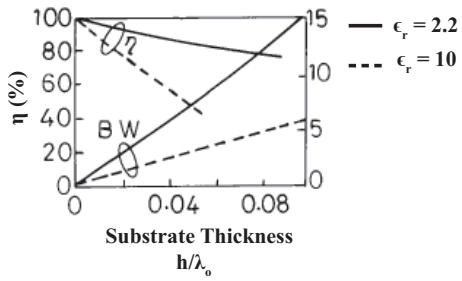

Figure 8: (a) Square patch antenna percentage bandwidth and efficiency variations versus substrate thickness h/λ_0 [10].

2.1.4 Polarization

One of the main advantage of using patch antenna is the polarization diversity that is offered through manipulating feeding position to excite different orientation of surface currents. The patch antenna can offer a linear (horizontal/vertical), ± slant 45° and left/right-hand CP. The polarization is decided based on the feeding point

and the topology of the antenna. In the simplest square patch antenna feeding point in the centerline of the patch and along one of the sides produces linear polarization along this side. Fig 9 displays an example of a dual fed antenna, the F1 and F2 can be fed separately inducing a linear polarization (F1: vertical and F2 horizontal). Making an offset 90° phase between these two feeds will result in circular polarization, the orientation will depend on the offset direction (±90°). Fig. 10 shows a different type of circular polarized antenna through optimizing the design of the patch itself.

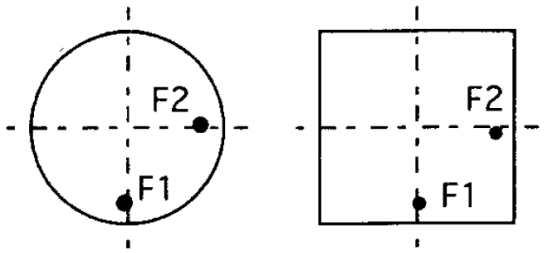

Figure 9: Dual fed circular and rectangular patches [9]

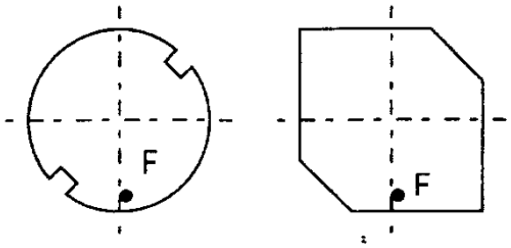

Figure 10: Single fed dual polarized patch antennas [9]

2.1.5 Multi-band

Some application require a multi band operations, patch antenna has a capability of operating in multi band through different techniques, such as; stacking the antennas, placing the antennas next to each other or excite different modes through the same patch by loading the patch with slots or shorting pins. Fig. 11 displays an example of a slotted antenna operating at 555 MHz and 1420 MHz with frequency ratio of 2.55.

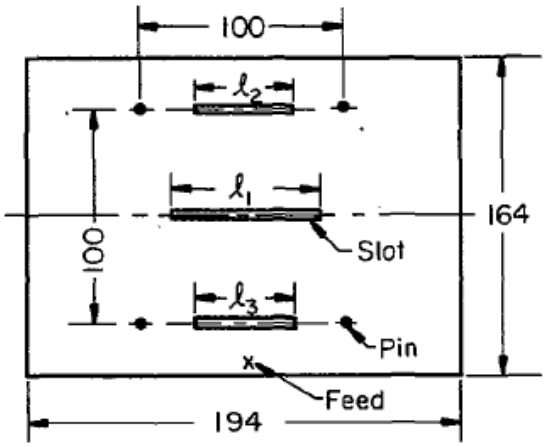

Figure 11: Single fed dual polarized patch antennas [11]

2.1.6 Antenna array

Patch antennas can be structured in a linear or planner array that provides better gain and can be used to beam scan and has a steering capability. The feeding strategy (the power and the phase) for each antenna decides the over all radiation pattern of the array, which is determined according to the required application. Fig. 12 displays a series fed linear patch antenna. Mutual coupling between antenna elements decides the spacing and the size of the array, according to the design goals the mutual coupling level is chosen. MIMO antenna arrays are different than the phased arrays in terms of the feeding as each antenna is fed independently.

Figure 12: Series fed linear patch antenna array [10]

2.2 Massive MIMO antenna array

Patch antenna has been utilized successfully to build a massive MIMO antenna arrays. The massive MIMO architecture depends mainly packing a high number of antenna elements in the targeted area with a specific threshold of mutual coupling between the elements. Several testbeds [12, 13] were designed to exploit the characteristics of the massive MIMO arrays through conducting channel measurements. Fig 13 shows an example of cylindrical stacked array of 64 elements and another T-shaped antenna array of 160 elements used by university of Lund.

(a) Cylindrical antenna array, 64 elements. [12]

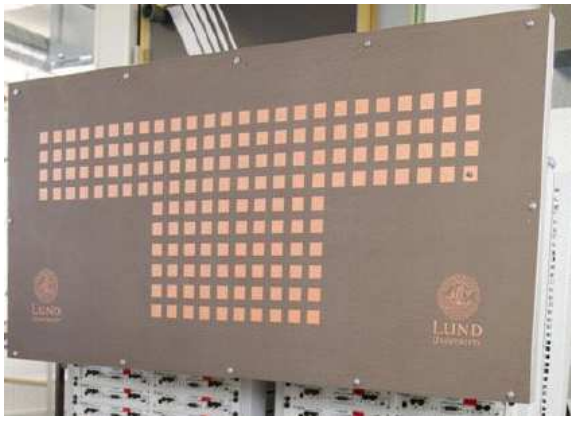

(b) T-shaped antenna array, 160 elements. [13]

Figure 13: Massive MIMO testbeds.

For practical applications, a more compact antenna arrays have been designed for massive MIMO purposes such as the turning torso [14] in Fig. 14 (a), which is a dual polarized array works at 3.7 GHz with an input matching bandwidth of 100 MHz. Another design presented in [15] offers another 8 × 8 miniaturized antenna array using CO_2Z hexaferrite substrate. Moreover, a cross array was designed using patch antennas in [16], it is a 33 × 33 elements operating at 77 GHz over a bandwidth of 3 GHz. According to the paper survey conducted at the beginning of the research all the current designs has a bandwidth ≤ 300 MHz and mostly operating on single frequency band.

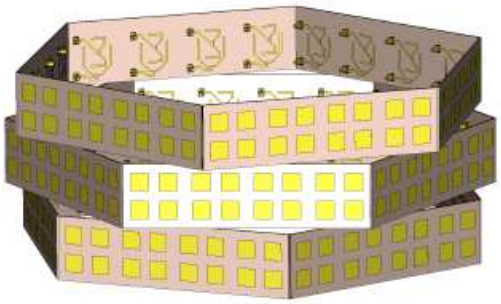

(a) Turning torso antenna array, 288 elements

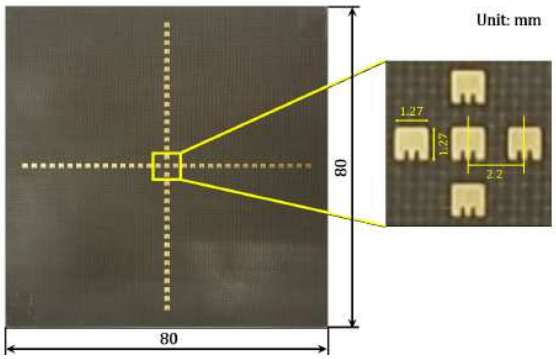

(b) Cross array, 33 × 33 elements

Figure 14: Compact massive MIMO antenna designs.

2.2.1 Design criteria

As discussed earlier a choice of a suitable substrate is crucial to assure a full functioning patch antenna. According to the design goals specified in the

introduction chapter, a multi-band patch antenna is required to operate on both 5.4 GHz and 15 GHz, such a design should be allocated on the same substrate as a same radiating element radiating on multi band or an antenna sub array. It is quite difficult to optimize a single element operating at a high frequency ratio as in this case (frequency ratio ≈ 3), so it was chosen to have a sub array of different elements operating on different frequency bands. A wide band response is also required as part of the design goal (≥ 320 MHz), relating to the percentage bandwidth it is easy to achieve a wide band response for the 15 GHz element, however, to apply bandwidth improvement techniques to the 5.4 GHz element, e.g. (increase the substrate thickness h) that would affect the radiation efficiency of the 15 GHz element as the higher frequency exhibits high dielectric losses. The upcoming chapter will introduce a reference design and its improvement to reach the design goals.

3 Design

3.1 Methodology

3.1.1 Simulations

All the simulations have been conducted using CST MWS 2015 [17]. The parameters were adjusted as the following: frequency range (3 GHz to 17 GHz), the boundaries were selected to be open (add space) in all directions, all the metal material was considered as copper (annealed) with a thickness $t = 0.02$ mm. RT8570 (lossy) with a thickness of 1.575 mm is selected as the substrate for the antenna array design. All the patch antenna feeding was considered as coaxial feed with inner cylindrical conductor diameter of 1.3 mm and outer shell of a diameter 4 mm. The coaxial dielectric material was chosen to be Teflon (lossy) with $\epsilon_r = 2.1$.

3.1.2 Coordinate system

Cartesian coordinates has been used to represent the antenna dimensions in free space. Fig. 15 shows the top and side view of a patch antenna.

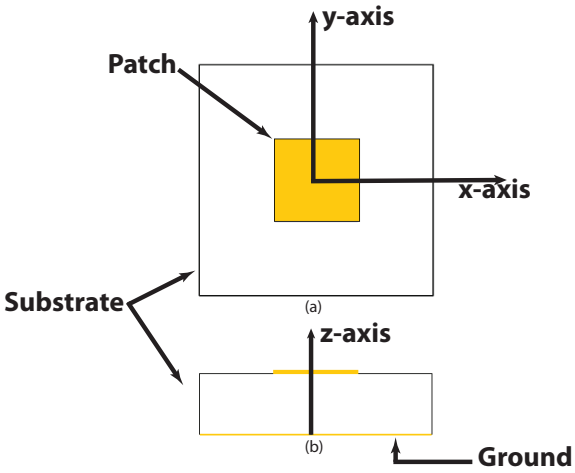

Figure 15: (a) Top view. (b) Side view.

For the radiation pattern, spherical coordinates are used along to describe the 2D radiation pattern cuts and angles. E-plane is defined as the plane along the feeding axis, in this case would be XZ-plane in Cartesian coordinate and the cut of $\varphi = 0°$ and θ is plotted. Accordingly, H-plane will be defined as YZ-plane in Cartesian coordinates and represented as the cut of $\varphi = 90°$ and θ is plotted.

3.2 Reference Design

The reference design is a cross patch sub array based on [18]. The design was optimized through (*how to cite the special assignment*) to fit the desired dual band requirement. The substrate used is a Rogers RT5870 with $\epsilon_r = 2.33$ and a height of

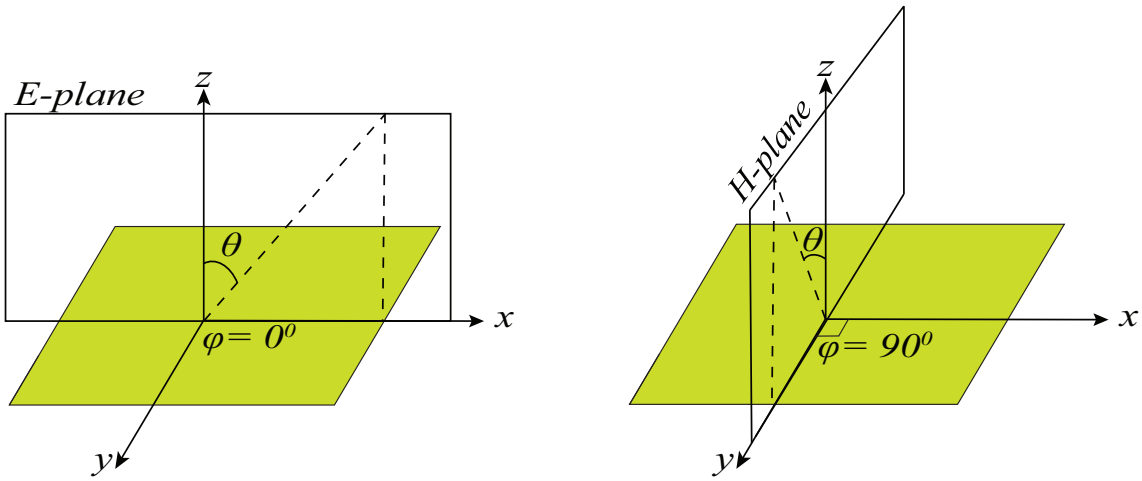

(a) E-plane in cartesian and spherical coordinates

(b) H-plane in cartesian and spherical coordinates

Figure 16: Radiation pattern coordinate perspective

1.575 mm, the height of the substrate choice is chosen to guarantee an adequate bandwidth for the lower frequency band ($f_{low} = 5.4$ GHz) and to assure a low radiation losses for the high frequency band ($f_{high} = 15$ GHz). The reference design fits the design goals in terms of the required input matching bandwidth (≥ 320 MHz) as well as the number of the elements for the assigned space as it has 48 elements of 5 GHz and 63 of 15 GHz elements (the design goal was ≥ 32 elements)

3.2.1 Unit element

The unit element operates at dual band; 5.4 GHz and 15 GHz. The unit element is a cross patch sub array as the cross patch is operates at 5.4 GHz while the sub array of four square patches antennas operates at 15 GHz as shown in Fig 17. The numbers represent the feeding port numbering and the circles defines the feeding position of the coaxial feed.

The 5.4 GHz cross patch patch can achieve an input matching bandwidth of ≈ 370 MHz (6.8% B.W) this is due to the cuts of the edges of the rectangular patch to form the cross shape which introduced more inductive response and and increased the bandwidth. The coupling level between the elements at the required band is ≤ -10 dB. For the 15 GHz the input matching bandwidth was ≥ 4 GHz (26.7% B.W). Fig. 18 shows the 5 GHz input matching and Fig. 19 shows the input matching of the 15 GHz, ports 2/4 and 3/5 are exactly the same due to the symmetric design.

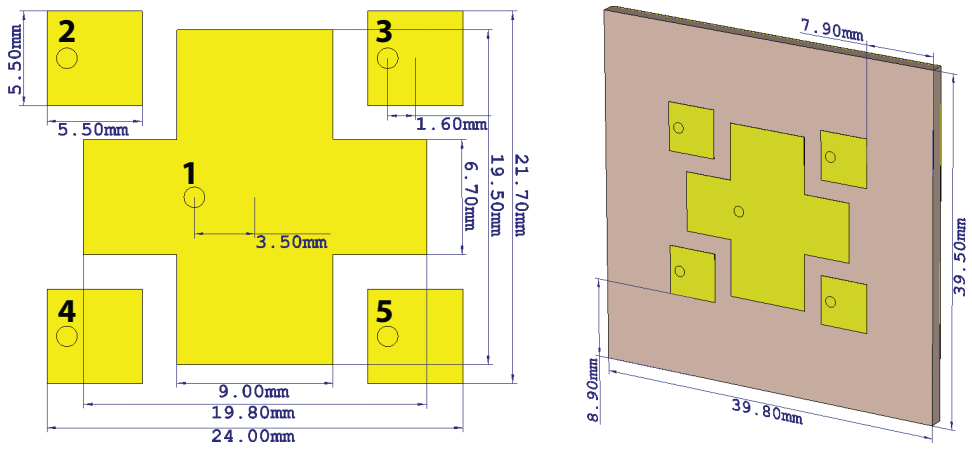

Figure 17: Cross patch sub array [18]

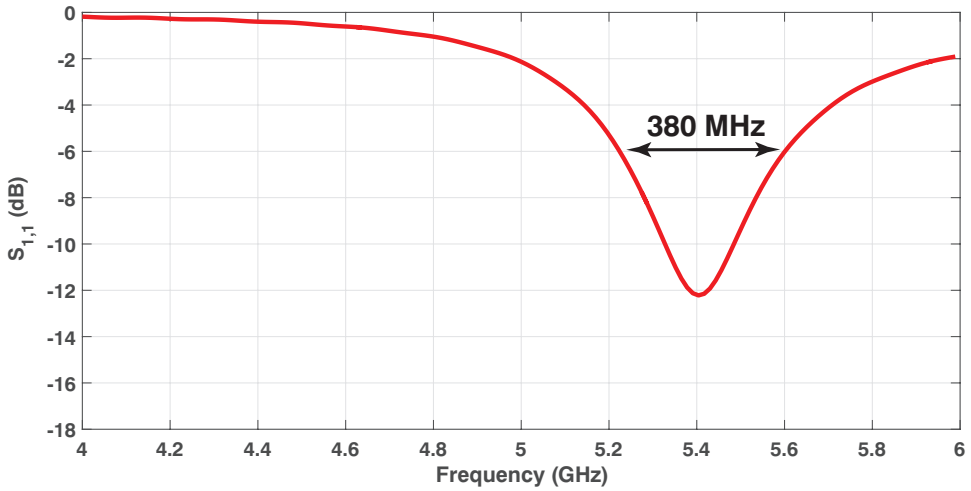

Figure 18: Simulated input matching level for 5.4 GHz cross patch

The coupling level between each element is displayed in Fig. 20 and due to the symmetric design the curves coincide e.g. $S_{4,3} = S_{5,2}$. The required bands are highlighted for the 5.4 GHz and the 15 GHz shows coupling level ≤ -10 dB.

The radiation pattern is presented in three different cuts, E-plane, H-plane and the azimuth plane respectively. The azimuth plane is plotted where $\theta = 90°$ and φ is plotted. Fig. 21 shows the radiation pattern of the 5 GHz cross patch antenna with gain of 7.6 dBi. Fig. 22 shows the radiation pattern of the 15 GHz antenna of patch number 2 as referred in Fig. 17 and it has a gain of 7.0 dBi.

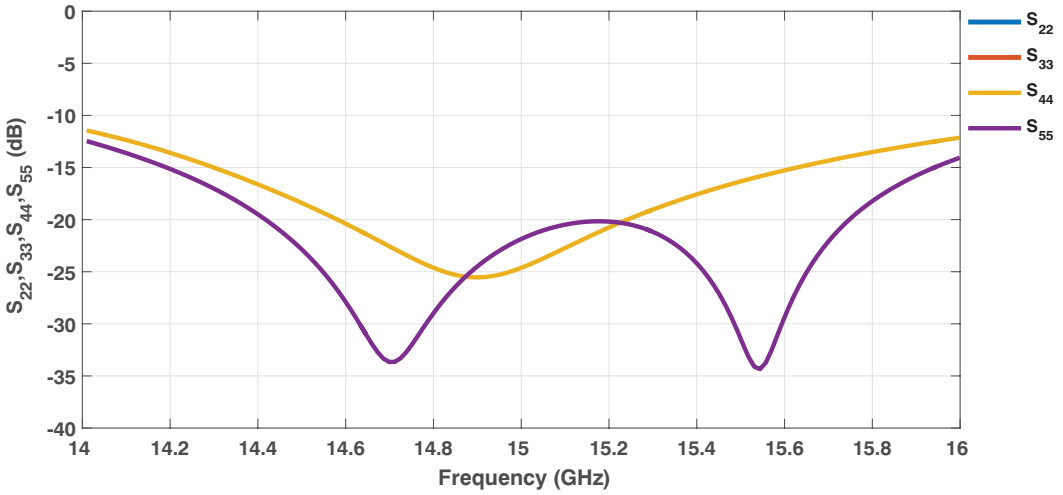

Figure 19: Simulated input matching level for 15 GHz square patch

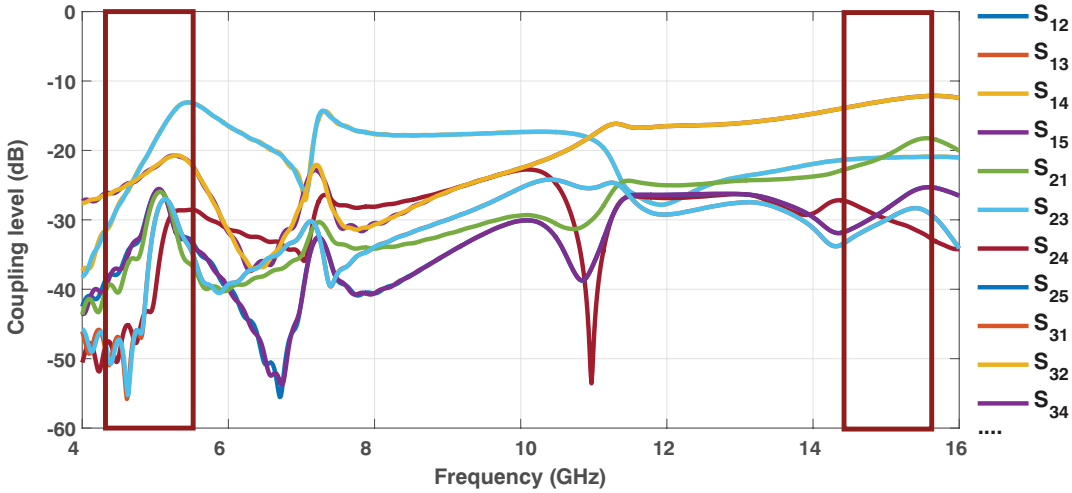

Figure 20: Coupling level between all elements, the desired bands are highlighted

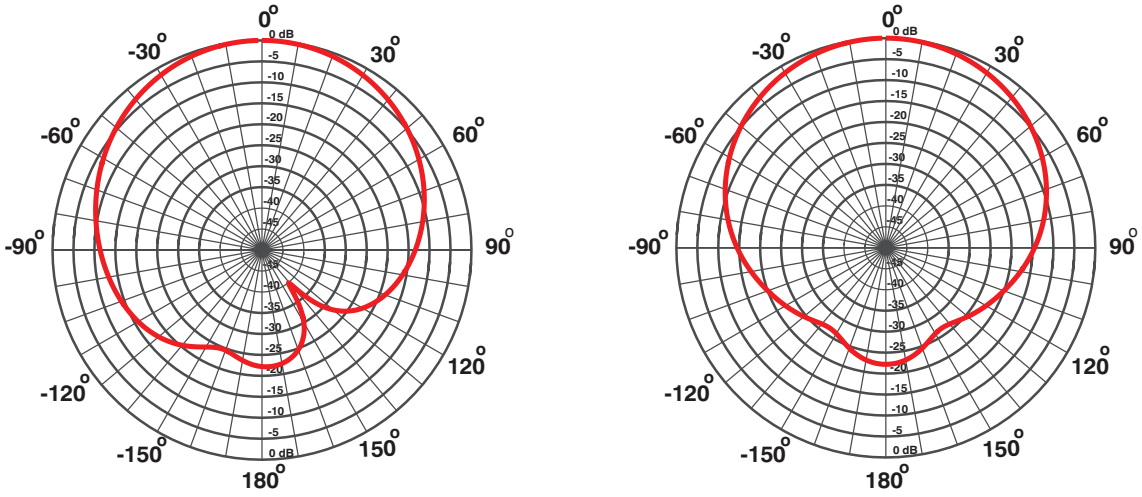

(a) E-plane (b) H-plane

Figure 21: Radiation pattern of the 5.4 GHz cross patch antenna

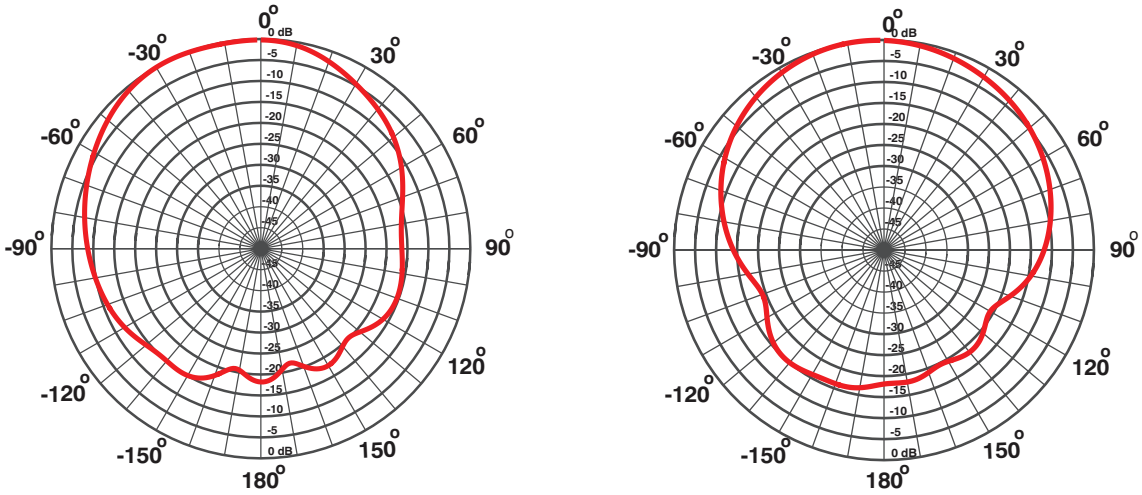

(a) E-plane (b) H-plane

Figure 22: Radiation pattern of the 15 GHz square patch antenna number 2

3.2.2 2×2 Array

An array of 2×2 is developed through duplicating the cross patch and optimizing the position of the square patch as shown in Fig. 23. The spacing between the elements is optimized as the horizontal spacing is 2.4 mm and the vertical spacing is 0.4 mm to acquire the required coupling level.

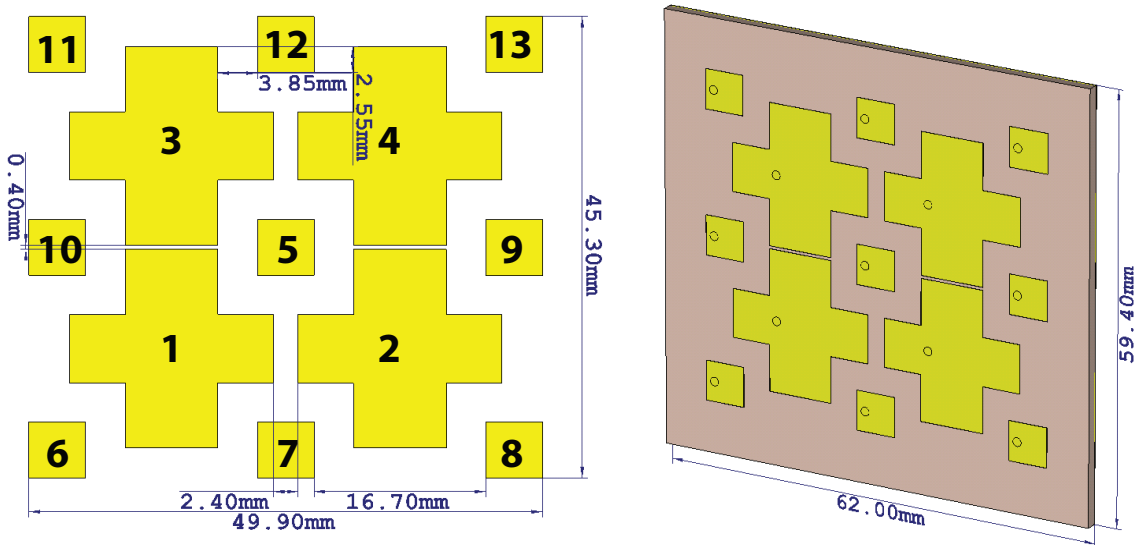

Figure 23: 2×2 antenna array

The input matching level of the four 5.4 GHz cross patches is shown in Fig. 24 the −6 dB bandwidth is ≈ 370 MHz. The input matching level of the 15 GHz square patch antenna is shown in Fig. 25 the −6 dB bandwidth is ≈ 2 GHz.

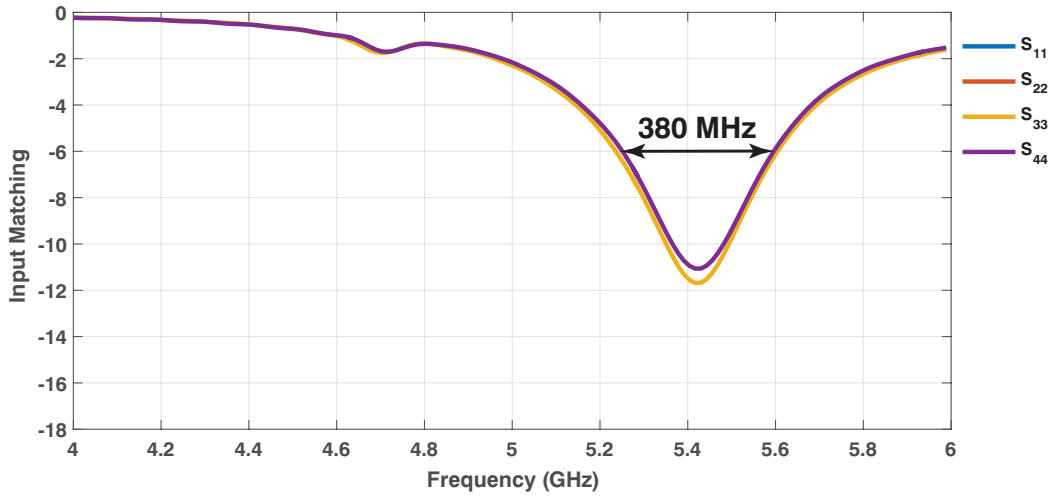

Figure 24: Input matching of the 5.4 GHz cross patches

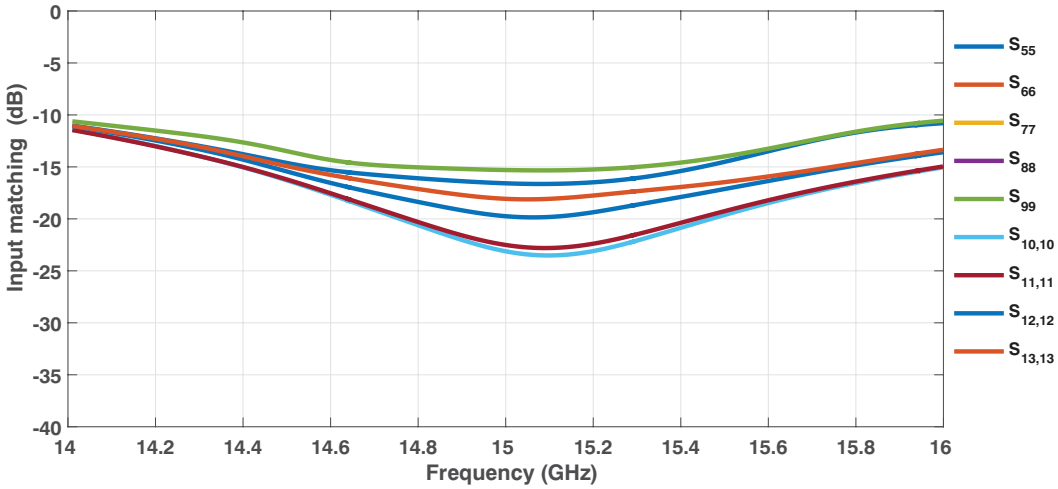

Figure 25: Input matching of the 15 GHz square patches

The coupling level between all the array elements is shown in Fig. 26. Due to the symmetric design most of the coupling curves coincide. The highlighted boxes shows the interested bandwidth (corresponding to the input matching bandwidth).

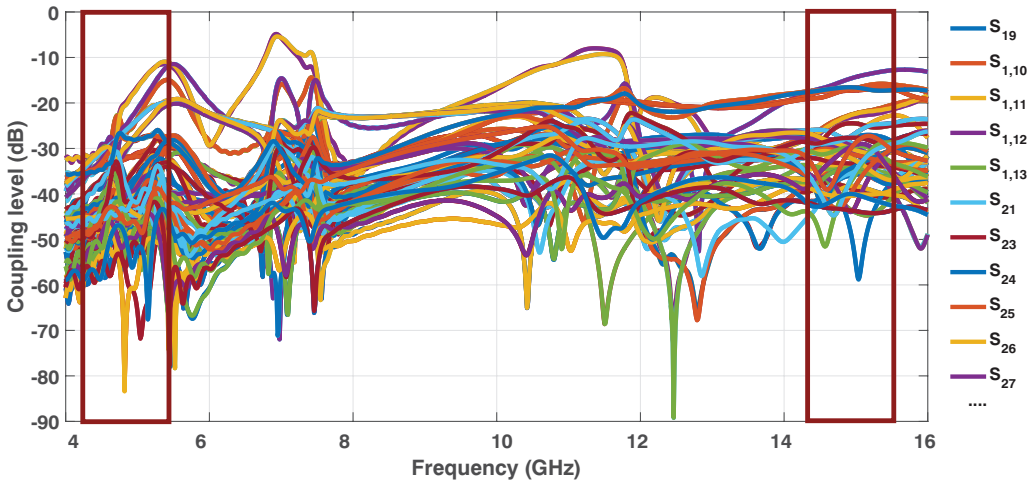

Figure 26: Coupling between all antenna array elements

3.2.3 Reference Array

The reference antenna array shown in Fig. 27. The array is composed of 6×8 (48) 5.4 GHz cross patch antennas and 7×9 (63) 15 GHz square patch antennas.

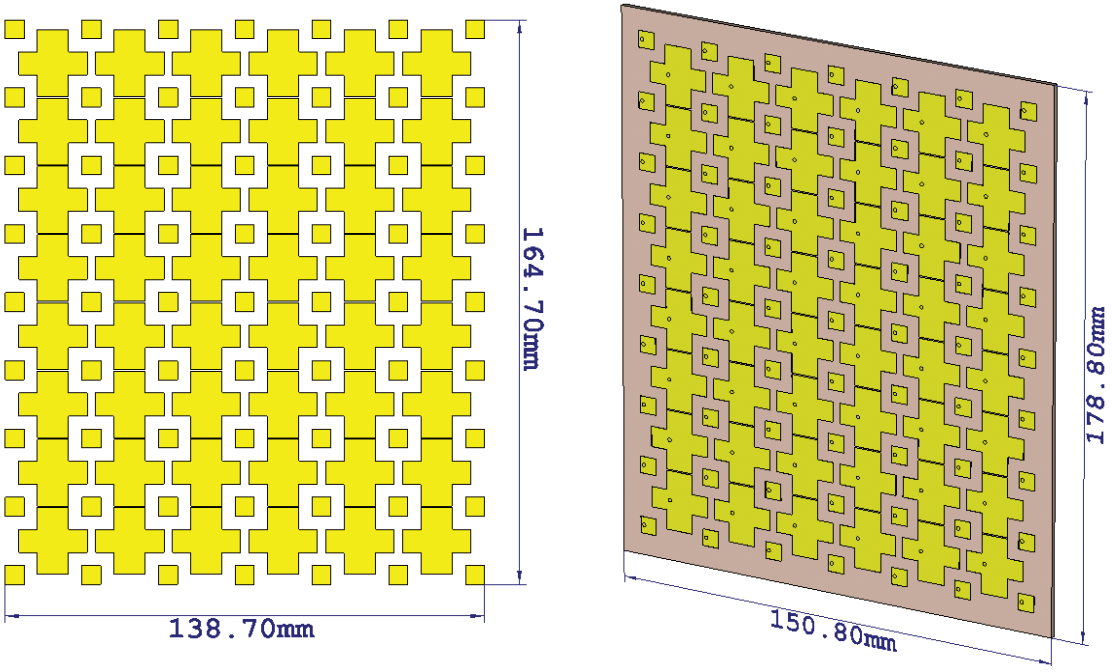

Figure 27: Antenna Array

In conclusion, the reference antenna fulfill the design goals in terms of number of elements in the defined space (150 mm × 180 mm) and in terms of bandwidth. However, the polarization criteria was still an issue as small size of the 15 GHz square patch antennas (5.5 mm × 5.5 mm), it is impractical to have a dual feed on the same patch as there is no commercial connectors can fit in such a small space. Moreover, the 5.4 GHz cross patch, the simulation showed the possibility of having a dual polarized cross patch, however, there is no small size of connectors that can be placed at this short distance. Improvements to achieve design goals will be discussed in the upcoming subsection.

3.3 Improved Design

The reference design did not fulfill the dual polarization requirement, due to the small size of the antennas and the available commercial connectors. For the 15 GHz patches has relatively high number (64 elements) it was suggested to decide the polarization according to the orientation of the patch instead of having a dual feed antenna. On the same hand, the 5.4 GHz dual polarization design was experimented, however it suffered from the close distance ports as well. It was advised to improve the bandwidth of the 5.4 GHz element and hence some designs were introduced.

3.3.1 Dual polarized cross patch antenna

The cross patch antenna was optimized to a symmetrical design to guarantee the same input matching response for both polarizations, Fig 28 shows the design. The input matching response and the mutual coupling between ports is plotted in Fig. 29 and it shows a narrower bandwidth of ≈ 270 MHz.

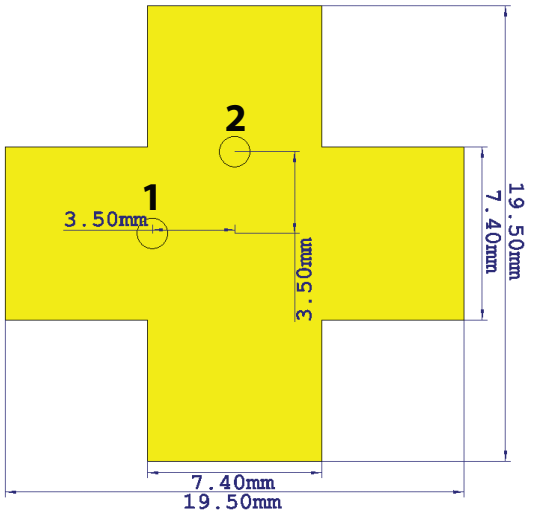

Figure 28: Dual polarized cross patch antenna

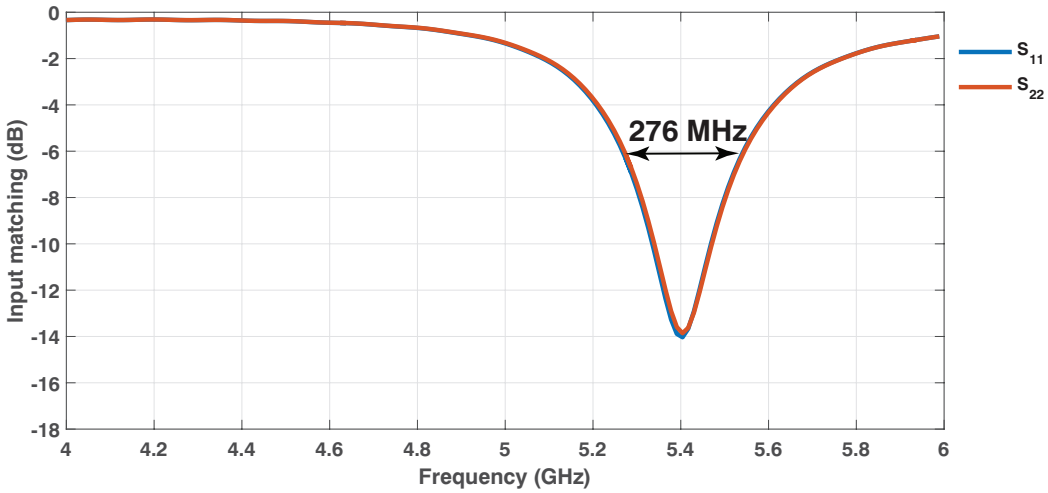

Figure 29: Input matching of dual polarized cross patch

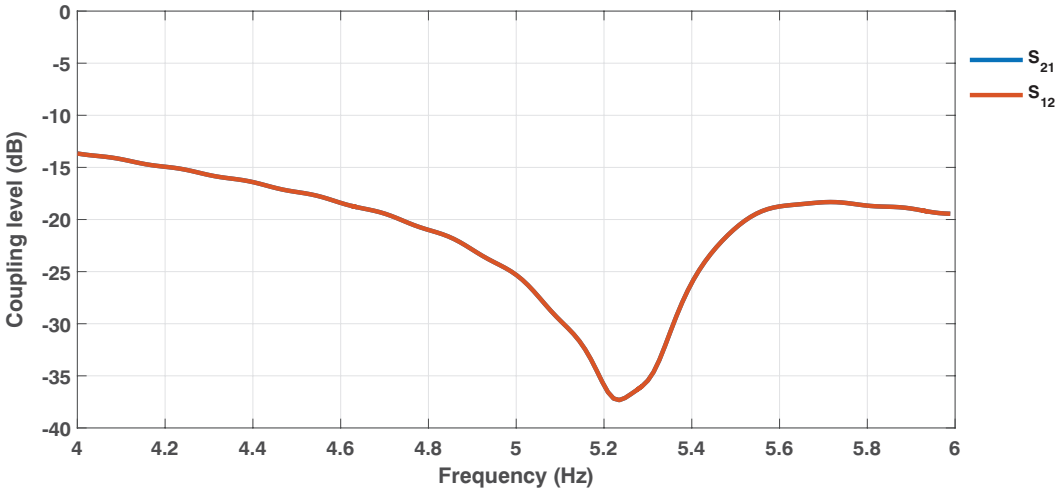

Figure 30: Coupling level between the two ports

The radiation pattern of co and cross polarizations in E-plane for port 1 (a) and port 2 (b) are illustrated in Fig. 31. The gain is ≈ 7 dBi and the cross polarization level is about -18 dBi for port 1 and -13 dBi for port 2.

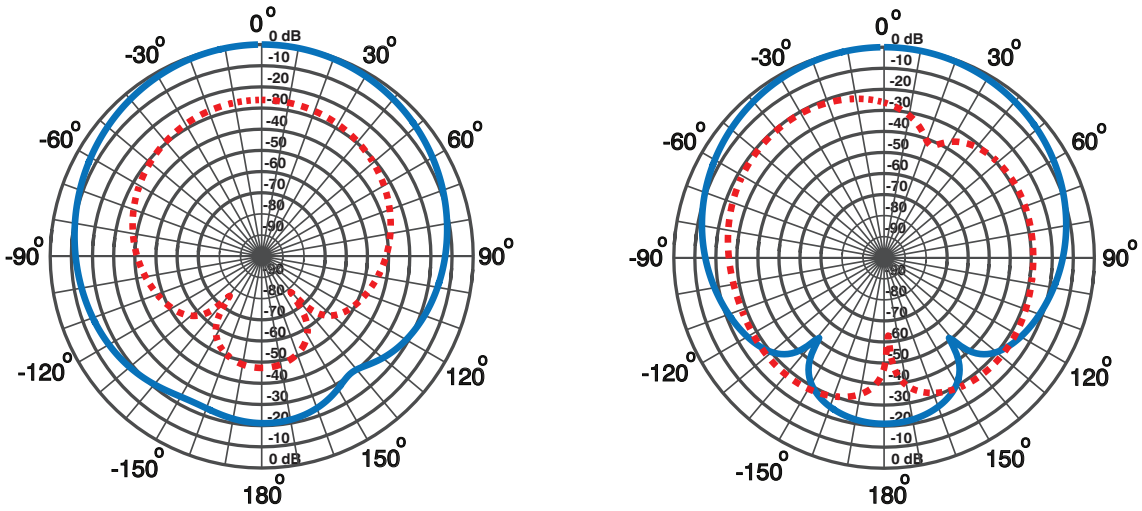

(a) Co and cross polarization pattern upon exciation of port 1

(b) Co and cross polarization pattern upon exciation of port 2

Figure 31: Co and cross polarization. (Blue) co, (red) cross

This design could not be realized as the distance between the two ports is too close and there is no commercial connector can fit into this space.

3.3.2 U-slot cross patch antenna

Inspired by [19], to achieve higher frequency, an attempt to have a cross patch antenna with a U-slot was simulated, the design and the dimensions are shown in

Fig. 32, the circle represent the feeding position from the center. The results for the input matching response are shown in Fig. ??. The design achieved an input bandwidth of ≈ 480 MHz.

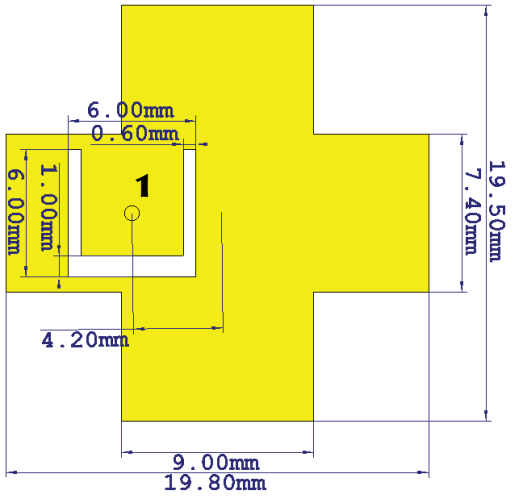

Figure 32: A cross patch antenna with a U-slot

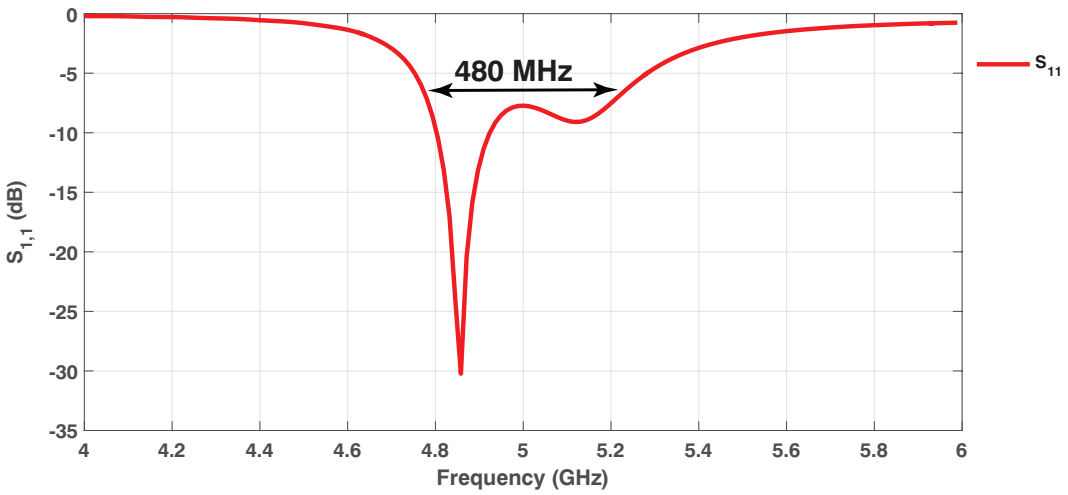

Figure 33: Input matching of the U-slot cross patch antenna

The radiation pattern of the antenna is displayed in Fig. 34. It has a gain of 7.6 dBi. In this case the dual polarization property cannot be achieved as the patch space is not enough to accommodate two U-slots at the same time.

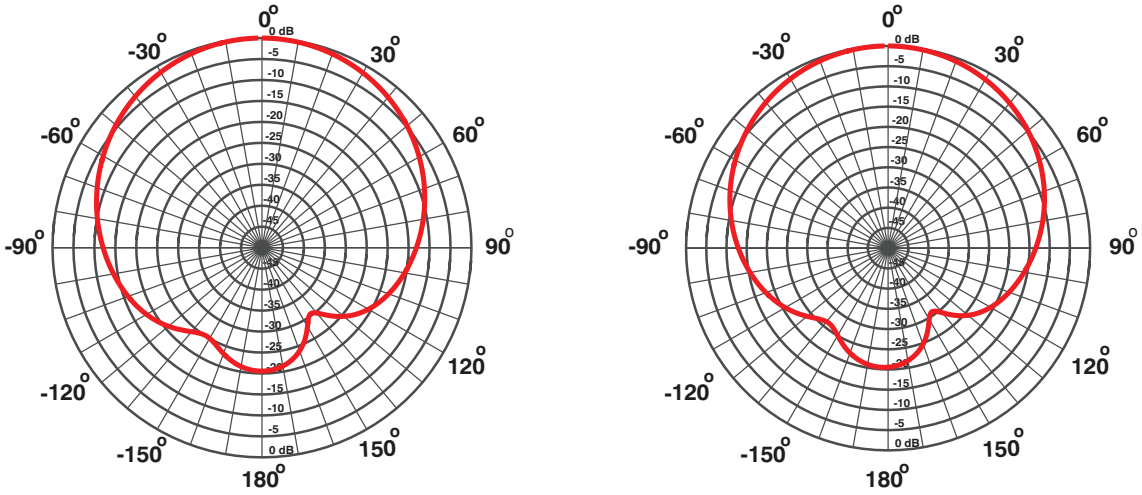

(a) E-plane

(b) H-plane

Figure 34: Radiation pattern of the 5 GHz U-slot cross patch antenna

4 Prototype and measurements

4.1 Prototype

A prototype of the reference antenna has been fabricated, a sample of the single unit, 2×2 array and the complete array are in Fig. 35. The measurement methodology and the measuring results are displayed in the upcoming subsections.

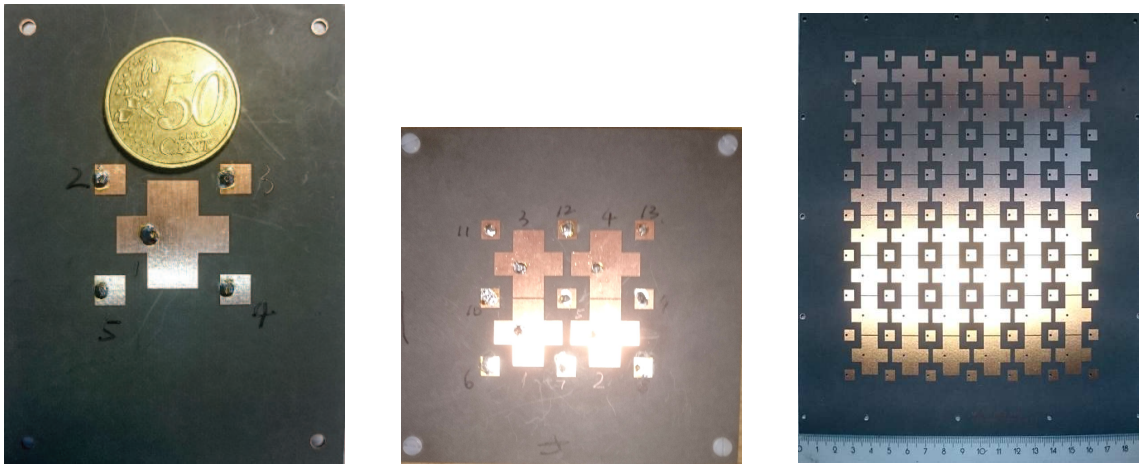

(a) A single unit compared to 50c size

(b) 2 × 2 array

(c) A full array

Figure 35: Reference design fabricated prototype

4.2 Methodology

4.2.1 S-parameters measurements

The S-parameters measurements were conducted using E5063A ENA Series Network Analyzer, Keysight Technologies [20]. Two calibration kits were used to calibrate the network analyzer at 5.4 GHz and 15 GHz. For the 5.4 GHz Keysight 85033D 3.5 mm calibration kit [21] has been used. For the 15 GHz Keysight 85052D 3.5 mm calibration kit [22] has been used. The network analyzer has been configured as follow:

- IF Bandwidth = 1 KHz.
- Number of points = 4001.
- Frequency range: (4 GHz - 6 GHz) & (14 GHz - 16 GHz).

4.2.2 Radiation pattern

The radiation pattern measurements were conducted at Radio Science and Engineering department at Aalto University anechoic chamber, the reference

antenna for the 5 GHz is a quad-ridged horn and an E/H planes horn antennas were used to measure the 15 GHz.
The measurements are divided into two groups, S-parameters measurements and radiation pattern for each frequency band.

4.3 Measurements

4.3.1 S-parameters

The 5 GHz measurements were conducted using two designs, single element Fig. 35 (a) to measure the input matching of the patch and 2 × 2 array Fig. 35 (b) to measure the coupling level between the 5.4 GHz cross patches. The results were collected and compared to the simulations. The S-parameters of the single element is displayed in Fig. 36. The 2 × 2 measured mutual coupling between neighbor patches at 5.4 GHz. The results of S_{21}, S_{31} and S_{41} (refer to Fig. 23 for port numbering) are displayed in Fig. 37.

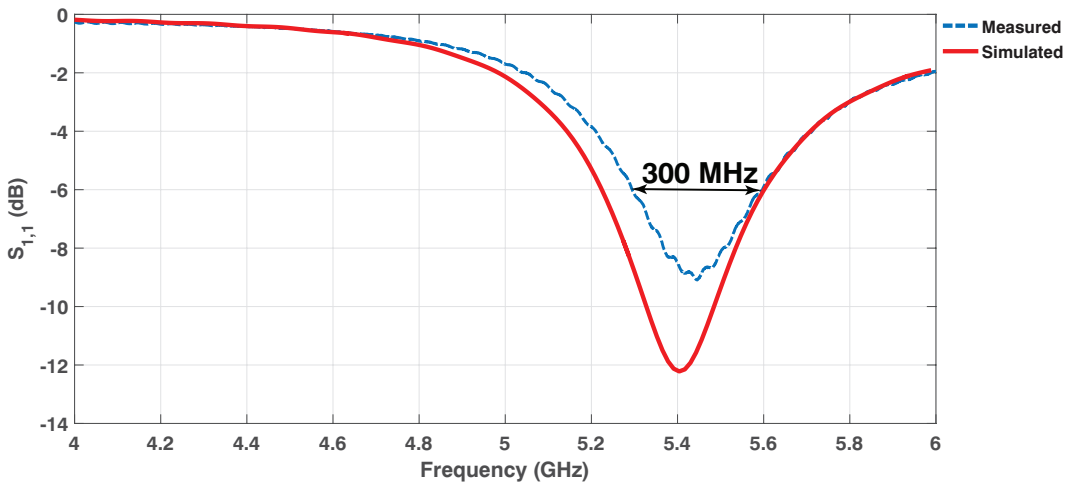

Figure 36: Input matching for port 1 ($S_{1,1}$) comparison between simulated (red) and measured (blue) results

For the input matching S_{11} there is a -20% less bandwidth than the simulated results this is assumed to be the inductive effect of the coaxial feed as it may increase the quality factor and reduce the bandwidth. For the mutual coupling curves, the measured results fits the simulated curves with the same trend, however, there exist ripples outside the interested bands and it is claimed that these ripples is a result of the reflection of the measuring environment.
The input matching for the 15 GHz square patch antenna were measured using the single unit. According to the simulations and due to the symmetrical shape port 2 and port 4 are identical as well as port 3 and port 5. Fig. 38 shows the measured input matching $S_{4,4}$ and $S_{5,5}$ compared to the simulated.

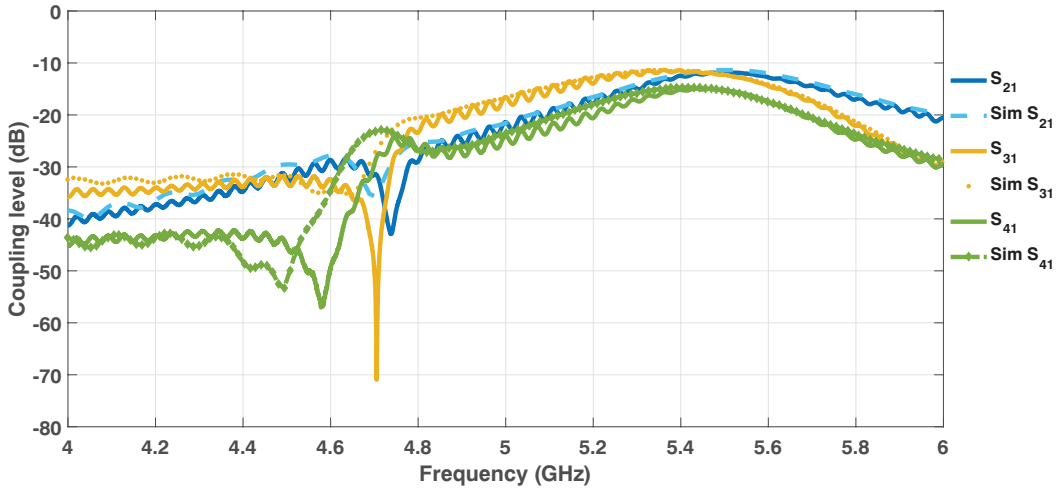

Figure 37: 5.4 GHz mutual coupling between port 1 and the other three ports 2,3 and 4.

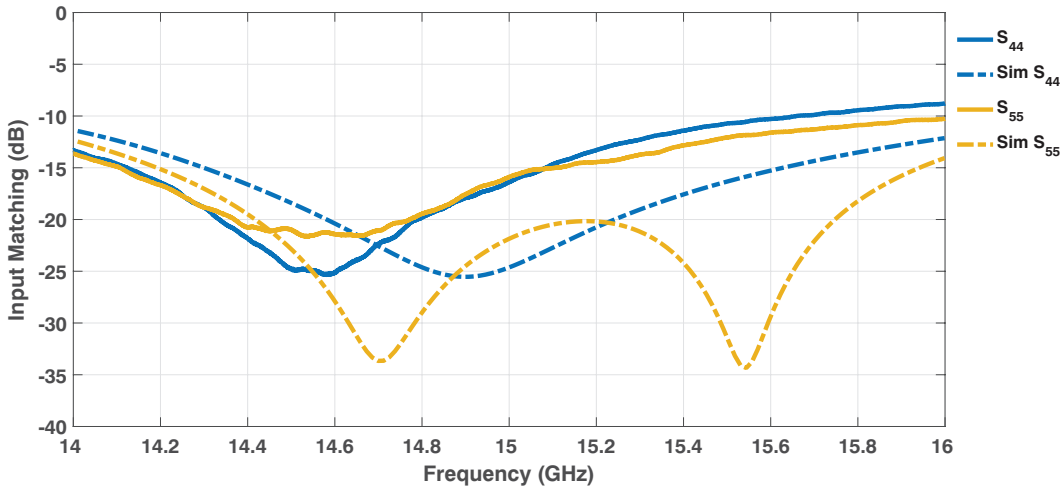

Figure 38: 15 GHz square patch input matching comparison for port 4 and port 5. (- - -) Simulated. (——) Measured

The mutual coupling were measured through the 2 × 2 array. Some results are displayed for $S_{11,5}$, $S_{12,10}$ and $S_{12,11}$ in Fig. 39.
For the input matching there is a 500 MHz shift in the response for port 2 and port 4. For port 3 and 5 the response is different than the simulation however it sustain an acceptable result of input matching ≤ -6 dB. The frequency shift is assumed to be due to the poor soldering and the inductive characteristics of the coaxial feed that may shift the resonance frequency. The mutual coupling between the neighboring ports is ≤ -10 dB over the required band, however the coupling level of the measured patches is less than the simulated one by almost 5 dB (e.g. for $S_{11,5}$ at 15.2 GHz the simulated ≤ -35 dB, measured = -35 dB).

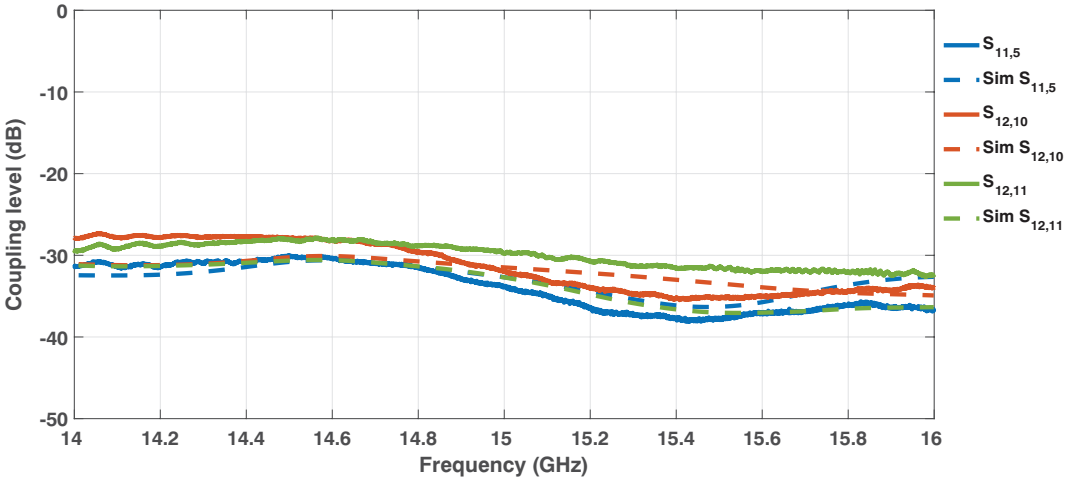

Figure 39: 15 GHz mutual coupling between neighboring ports. (- - -) Simulated. (——) Measured

4.3.2 Radiation patterns

Radiation pattern measurements were conducted using the 2 × 2 array, Fig. 40.

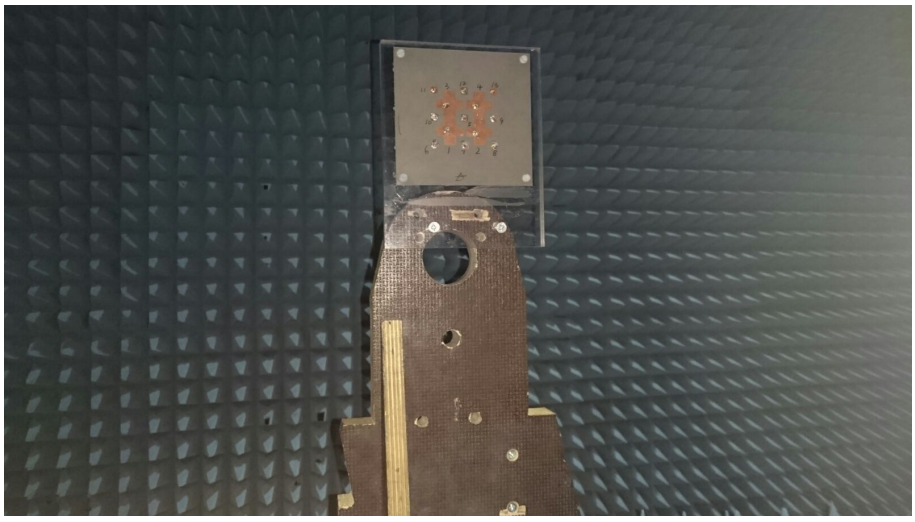

Figure 40: 2 × 2 array in the anechoic chamber.

For the 5.4 GHz, a quad rigid horn is used as illustrated in Fig. **??** (a), the antenna has dual feeding ports as shown in Fig. 41 (b). In this case only E-Plane was measured and the horn antenna was fed vertically and horizontally to obtain the co and cross polarization. Fig. 42 shows the radiation pattern of the 5.4 GHz cross patch pattern for patch 1 and patch 4.

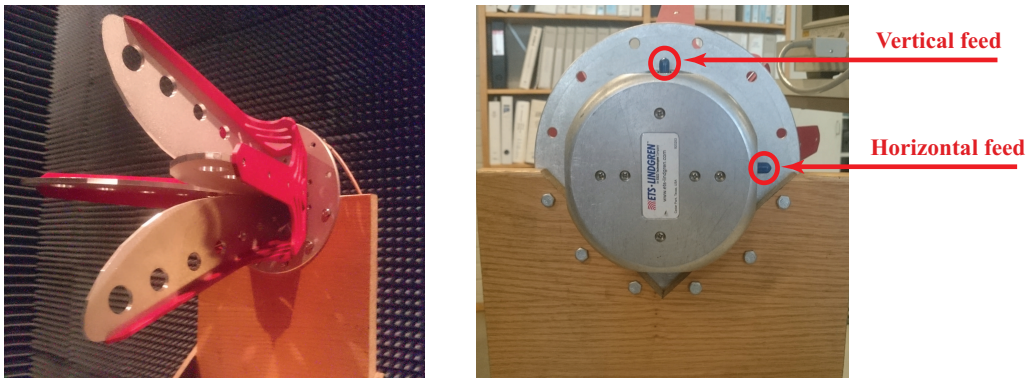

Figure 41: Quad Rigid horn antenna. (a) Front view. (b) back view.

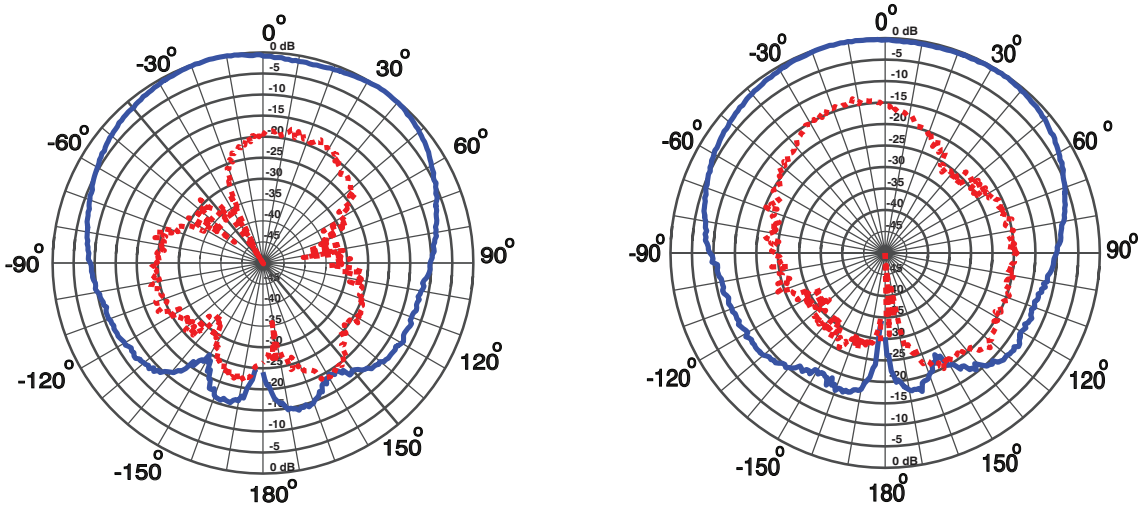

(a) E-plane of 5.4 GHz cross patch, port 1

(b) E-plane of 5.4 GHz cross patch, port 4

Figure 42: E-plane radiation pattern for 5.4 GHz cross patches 1 and 4. (Blue) co polarization, (red) cross polarization

For the 15 GHz measurement, patch number 5 was measured. The feeding antennas used were an identical co and cross fed horn antennas as represented in Fig. 43 (a). The different feeding port orientation is shown in Fig. 43 (b) and (c). E-plane and H-plane has been measured for the 15 GHz and displayed in Fig. 44. Due to some technical issues in the anechoic chamber, small number of points were taken to be plotted and it is seen as rough lines in the radiation pattern plot.

Figure 43: 15 GHz horn antenna. (a) Front view. (b) Cross fed. (c) Co fed.

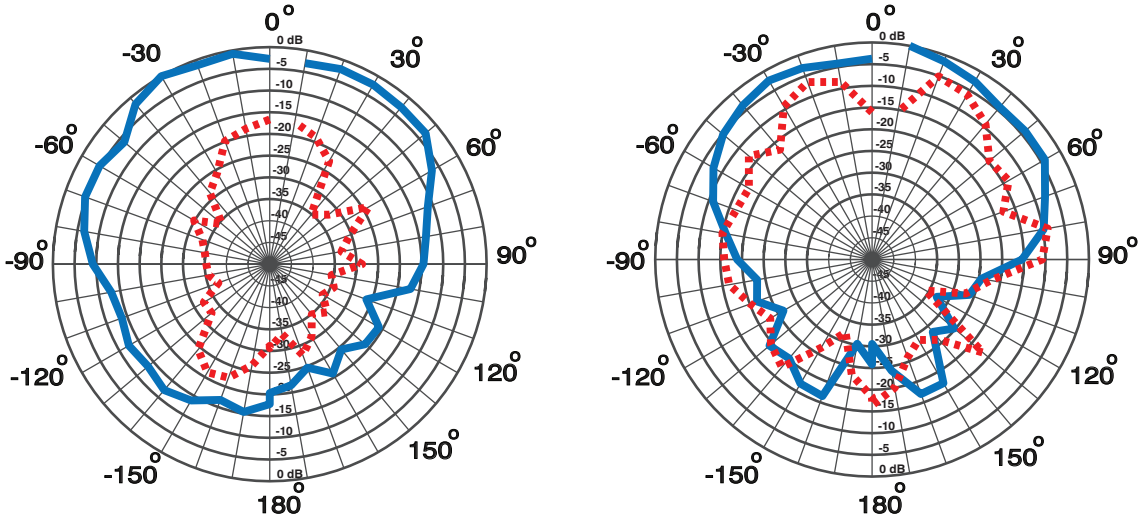

(a) E-plane (b) H-plane

Figure 44: Radiation pattern of 15 GHz patch number 5. (a) E-plane. (b) H-plane. (Blue) co polarization. (Red) cross polarization

5 Conclusion & Future work

In conclusion, a patch antenna array has been designed and fabricated to serve as massive MIMO antenna array. The dual polarization requirement could not be realized due to the small distance between the ports in reference to the available coaxial connectors. The reference design fits the requirement for size versus number of antenna elements, as it accommodate up to 111 elements for both frequency bands. The mutual coupling between the elements matched the design goals criteria (≤ -10 dB) for all neighboring elements for all bands. The simulation showed a good input matching bandwidth response (370 MHz over $\leq$ - 6 dB), however the measured bandwidth was about -20% less, this is may be due to the inductive effect of the coaxial connectors. There was a significant shift in the 15 GHz patches input matching response for center frequency ($\approx$ 500 MHz) and it is assumed to be due to poor soldering and the effect of the connectors.

The radiation pattern for the 5 GHz cross patch has been successfully measured and plotted. However due to technical difficulties at the department facility, the 15 GHz measurements could not be done, although different trials to do semi manual measurements was tried.

5.1 Future work

As the design gives open the door for more degree of freedom in terms of diversity (frequency and polarization). The polarization requirement should be considered to add a new level of performance. It is recommended to search for a more suitable dielectric substrate that can guarantee a good performance for such a high and low frequency difference.

The size can be reduce more by applying miniaturization techniques and it can be done through making the design on different layers for instance. Smaller antenna size resembles a high number of elements per required space which elevate the performance of the system.

References

[1] J. Sharony, *Introduction to MIMO - Theory and Application.* (March 31 2016 [Online] www.ieee.li/pdf/viewgraphs/introduction_to_wireless_mimo.pdf.

[2] T. Marzetta, "Massive MIMO: An introduction," *Bell Labs Technical Journal*, vol. 20, pp. 11–22, March 2015.

[3] T. Svantesson and A. Ranheim, "Mutual coupling effects on the capacity of multielement antenna systems," in *in Proc. 2001 IEEE Int. Conf. (ICASSP '01)*, vol. 4, pp. 2485–2488, Feb. 2001.

[4] X. Liu and M. E. Bialkowski, "Mutual coupling on MIMO channel estimation and capacity," *Int. J. of Antennas Propag.*, vol. 2010, pp. 9, Article ID 306173, Jan. 2010.

[5] P. N. Fletcher, M. Dean, and A. R. Nix, "Mutual coupling in multi-element array antennas and its influence on MIMO channel capacity," *Electronics Lett.*, vol. 39, pp. 342–344, Feb. 2003.

[6] A. A. Abouda and S. G. Häggman, "Effect of mutual coupling on capacity of MIMO wireless channels in high SNR scenario," *Progress In Electromagn. Research*, vol. 65, pp. 27–40, 2006.

[7] X. Li and Z.-P. Nie, "Mutual coupling effects on the performance of MIMO wireless channels," *IEEE Antennas Wireless Propag. Lett.*, vol. 3, pp. 344–347, Dec. 2004.

[8] G. Deschamp, "Microstrip microwave antennas," in *3rd USAF Symp. on Antennas*, 1953.

[9] R. Garg, *Microstrip Antenna Design Handbook.* Antennas and Propagation Library, Artech House, 2001.

[10] G. Kumar and K. Ray, *Broadband Microstrip Antennas.* Artech House antennas and propagation library, Artech House, 2003.

[11] B. Wang and Y. Lo, "Microstrip antennas for dual-frequency operation," *IEEE Trans. Antennas Propag.*, vol. 32, pp. 938–943, Sep. 1984.

[12] X. Gao, F. Tufvesson, O. Edfors, and F. Rusek, "Measured propagation characteristics for very-large MIMO at 2.6 GHz," in *Proc. Asilomar Conf. Signals Syst. Comput.*, Pacific Grove, CA, USA, Nov. 2012.

[13] J. Vieira, S. Malkowsky, K. Nieman, Z. Miers, N. Kundargi, L. Liu, I. Wong, V. Owall, O. Edfors, and F. Tufvesson, "A flexible 100-antenna testbed for massive MIMO," in *Proc. Globecom Workshops (GC Wkshps)*, pp. 287–293, Dec. 2014.

[14] R. Ma, Y. Gao, C. Parini, and L. Cuthbert, "Dual-polarized turning torso antenna array for massive MIMO systems," in *2015 9th European Conf. on Antennas Propag. (EuCAP 2015)*, pp. 1–2, April 2015.

[15] Q. Zhang, Z. Chen, Y. Gao, C. Parini, and Z. Ying, "Miniaturized antenna array with Co2Z hexaferrite substrate for massive MIMO," in *2014 IEEE Antennas Propag. Soc. Int. Symp. (APSURSI)*, pp. 1803–1804, July 2014.

[16] T. Kwon, Y. Lim, B. Min, and C. Chae, "RF lens-embedded massive MIMO systems: Fabrication issues and codebook design," *Comput. Research Repository*, pp. 1–14, Oct. 2015.

[17] *CST - Computer Simulation Technology*. (Last visited March 31 2016) [Online] https://www.cst.com.

[18] C. Salvador, L. Borselli, A. Falciani, and S. Maci, "Dual frequency planar antenna at S and X bands," *Electronics Lett.*, vol. 31, pp. 1706–1707, Sep. 1995.

[19] A. Deshmukh and K. P. Ray, "Analysis of broadband variations of U-slot cut rectangular microstrip antennas," *IEEE Antennas Propag. Magazine*, vol. 57, pp. 181–193, April 2015.

[20] *E5063A ENA Series Network Analyzer*. (Last visited March. 31 2016) [Online] http://www.keysight.com/en/pdx-x202023-pn-E5063A/ena-series-network-analyzer.

[21] *85033D Calibration Kit, 3.5 mm*. (Last visited March. 31 2016) [Online] http://www.keysight.com/en/pd-1000000584%3Aepsg%3Apro-pn-85033D/calibration-kit-35-mm.

[22] *85052D Economy Mechanical Calibration Kit, DC to 26.5 GHz, 3.5 mm*. (Last visited March. 31 2016) [Online] http://www.keysight.com/en/pd-1000002018%3Aepsg%3Apro-pn-85052D/economy-mechanical-calibration-kit-dc-to-265-ghz-35-mm?cc=FI&lc=fin.